Electronic Supplementary Material (ESI) for Chemical Science.
This journal is © The Royal Society of Chemistry 2019

Supporting Information

Visualizing the Intracellular Particles and Precise Control of Drug Release Using an Emissive Hydrazone Photochrome

Xing Guo,[‡a] Baihao Shao,[‡b] Shaobing Zhou,*[a] Ivan Aprahamian*[b] and Zi Chen*[c]

[a] Key Laboratory of Advanced Technologies of Materials Ministry of Education, School of Materials Science and Engineering, Southwest Jiaotong University, Chengdu 610031, China. E-mail:
[b] Department of Chemistry, Dartmouth College, Hanover, New Hampshire 03755, United States. Email:
[c] Thayer School of Engineering, Dartmouth College, Hanover, New Hampshire 03755, United States.
‡ These authors contributed equally to this work.
* E-mail: zi.chen@dartmouth.edu; ivan.aprahamian@dartmouth.edu; shaobingzhou@swjtu.edu.cn

Table of Contents

1 General Methods

All reagents and starting materials were purchased from commercial vendors and used as supplied unless otherwise indicated. Methoxy poly (ethylene glycol) amine (mPEG-NH_2, molecular weight (MW): 5000) was purchased from JenKem Technology. (S)-Benzyl 3-(2,5-dioxooxazolidin-4-yl) propanoate (BLG-NCA) was purchased from Sigma-Aldrich. 2-Hydroxypyridine was purchased from Alfa Aesar. All experiments were conducted under air unless otherwise noted. Compounds were purified by column chromatography using silica gel (SiliCycle®, 60 Å, 230-400 mesh) as stationary phase and solvents mixtures used during chromatography were reported as volume ratios unless otherwise noted. Deuterated solvents were purchased from Cambridge Isotope Laboratories, Inc. and used as received. ^{1}H NMR and ^{13}C NMR were recorded on a 500 or 600 MHz NMR spectrometer, with working frequencies of 500.13 or 600.13 MHz for ^{1}H nuclei, and 125.8 or 150.9 MHz for ^{13}C nuclei, respectively. Chemical shifts are quoted in ppm relative to tetramethylsilane, using the residual solvent peak as the reference standard. ESI mass spectra were obtained on a Shimadzu LCMS-8030 mass spectrometer. Melting points were measured on an Electrothermal Thermo Scientific IA9100X1 digital melting point instrument. UV-Vis spectra were recorded on a Shimadzu UV-1800 UV-Vis spectrophotometer. A Photon Technology International QuantaMaster 4 spectrofluorometer outfitted with a LPS-100 lamp power supply and Xenon arc lamp housing, ASOC-10 electronics interface, MD-4 motor driver control, and a model 914D photomultiplier detector system was used to collect fluorescence spectra of model compound **2**. Quantum yield of DMSO solution was measured using a Horiba model 914D photomultiplier detector system with a calibrated integrating sphere. The fluorescence emission spectra for the polymer (**LSP**) and nanoparticles (**LSNP**) were recorded on a fluorescence spectrometer (FluoroMax-3, JY-Horiba). Dynamic light scattering (DLS, Malvern Zetasizer) was used to measure the average size distribution and polydispersity of the nanoparticles. Transmission electron microscopy (TEM, JEOL Ltd., Japan) was used for imaging of nanoparticles observation (phosphotungstic acid was used in negative staining).

All the irradiation experiments on model compound **2**, and photostationary state studies of **LSP** were carried out using a stand-alone xenon arc lamp system (Model: LB-LS/30, Sutter Instrument Co.), which is outfitted with a SMART SHUTTER controller (Model: LB10-B/IQ, Sutter Instrument Co.) and a liquid light guide LLG/250. 340 (part number: 340HC10-25) and 442 (part number: 442FS10-25) nm light filters purchased from Andover Corporation were used in the irradiation experiments. The rest of the irradiation experiments on **LSP** and **LSNP** were done with escolite light coupled with 450 nm light filter for visible light irradiation and 3UV™-38 UV Lamp for UV light irradiation.

2 Experimental Section

2.1 Synthesis

Scheme S1. Synthesis of model compound **2**, and the light-switchable polymer **LSP**.

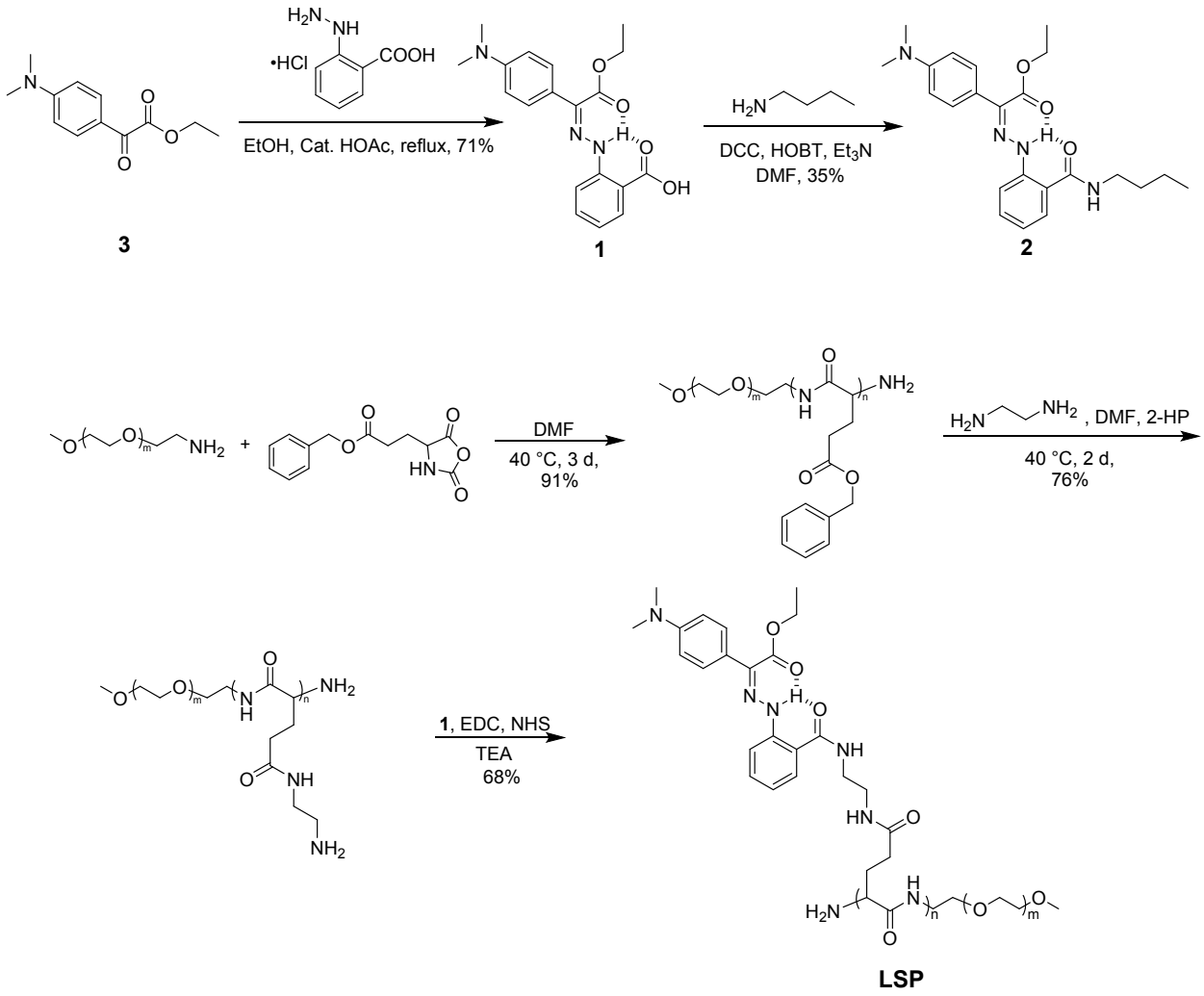

Synthesis of hydrazone 1

1: Ethyl 2-(4-(dimethylamino) phenyl)-2-oxoacetate (650 mg, 1.0 equiv.),[1] was added to a ethanol solution (25 mL) of 2-hydrazinobenzoic acid hydrochloride (608 mg, 1.1 equiv.) followed by the addition of catalytic amount of acetic acid. The reaction was left to reflux overnight. After cooling to room temperature, a large amount of water was added, and the precipitate was collected by filtration. Hydrazone **1** was obtained as a yellow powder (740 mg, 71 % yield; *Z*/*E* = 8/2). ^{1}H NMR (600 MHz, CD_2Cl_2) δ 13.23 (s, 1H), 8.06 (dd, *J* = 8.0, 1.6 Hz, 1H), 7.96 (t, *J* = 8.8 Hz, 1H), 7.63 (d, *J* = 8.8 Hz, 2H), 7.59 (t, *J* = 7.7 Hz, 1H), 6.97 (t, *J* = 7.5 Hz, 1H), 6.77 (d, *J* = 8.8 Hz, 2H), 4.48 (q, *J* = 7.1 Hz, 2H), 3.04 (s, 6H), 1.43 (t, *J* = 7.1 Hz, 3H) ppm; ^{13}C NMR (151 MHz, $CDCl_3$) δ 163.00, 150.44, 147.21, 135.61, 135.21, 131.66,

129.27, 124.14, 119.58, 119.41, 114.81, 114.48, 111.73, 61.40, 40.42, 14.29 ppm. Hi-Res MS (ESI): m/z found [M–H$^+$] for $C_{19}H_{22}N_3O_4^+$ 356.1613 (calcd. 356.1605).

Synthesis of model compound 2

2: *N*,*N*'-Dicyclohexylcarbodiimide (DCC; 87 mg, 1.5 equiv.) and 1-hydroxybenzotriazole hydrate (HOBt·H_2O; 57 mg, 1.5 equiv.) were added to a DMF solution (5 mL) of **1** (100 mg, 1.0 equiv.) and the reaction was left to stir at rt for 6 hours. *n*-Butylamine (36 μL, 1.3 equiv.) and triethylamine (59 μL, 1.5 equiv.) were added to the above mixture, which was stirred at 60 ℃ overnight. The mixture was diluted with water (20 mL) and extracted with ethyl acetate (20 mL × 3). The organic phase was washed with brine (30 mL) and dried over anhydrous Na_2SO_4. The solvent was removed under reduced pressure and the residue was subjected to column chromatography using dichloromethane/methanol (30:1 to 10:1). The obtained powder was further recrystallized from ethanol/water to afford **2** as a yellow powder (40 mg, 35 % yield). m.p. 145.2–145.7 ℃. ^{1}H NMR (500 MHz, CD_2Cl_2) δ 13.29 (s, 1H), 7.87 (d, J = 8.7 Hz, 1H), 7.56 (dt, J = 9.0, 3.1 Hz, 2H), 7.46–7.38 (m, 2H), 6.90 (td, J = 8.1, 1.2 Hz, 1H), 6.72 (d, J = 9.0, 3.1Hz, 2H), 6.17 (s, 1H), 4.42 (q, J = 7.1 Hz, 2H), 3.50–3.39 (m, 2H), 2.99 (s, 6H), 1.66–1.56 (m, 2H), 1.49–1.41 (m, 2H), 1.39 (t, J = 7.1 Hz, 3H), 0.97 (t, J = 7.4 Hz, 3H) ppm; ^{13}C NMR (151 MHz, CD_2Cl_2) δ 168.07, 162.94, 150.37, 144.97, 132.34, 132.19, 129.03, 126.61, 124.36, 119.60, 117.17, 114.73, 111.55, 61.21, 40.17, 39.53, 31.69, 20.18, 14.01, 13.57 ppm; Hi-Res MS (ESI): m/z found [M–H$^+$] for $C_{23}H_{31}N_3O_4^+$ 411.2387 (calcd. 411.2391).

Synthesis of Methoxy Poly(ethylene glycol)-*b*-Poly(benzyl-L-glutamate) (mPEG-PBLG) Copolymer

The mPEG-PBLG block copolymer was synthesized via ring opening polymerization of BLG-NCA initiated by mPEG-NH_2. Briefly, BLG-NCA (0.5 g, 1.9 mmol) was dissolved in dimethylformamide (DMF), and then added to a stirred DMF solution (3 mL) of mPEG-NH_2 (0.5 g, 0.1 mmol) under nitrogen. The mixture was reacted for 3 days at 40 ℃, and dialyzed (MWCO 7 kDa) against deionized water for purification. The mPEG-PBLG copolymer was obtained by freeze drying (91% yield).

Synthesis of mPEG-*b*-Poly(ethylenediamine-L-glutamate) (mPEG-PELG) Copolymer

The mPEG-PELG was synthesized through ammonolysis using excess ethylenediamine. Briefly, ethylenediamine (614 μL, 9.2 mmol) was added to a stirred DMF solution (3 mL) of mPEG-PBLG (0.8 g, 1.84 mmol of benzyl ester) under nitrogen. After the 2 d of reaction at 40 ℃, 10% acetic acid solution was slowly added to cooled (0 ℃) mixture, and then dialyzed (MWCO 3.5 kDa) against deionized water for purification. The mPEG-PELG copolymer was obtained by freeze drying (76% yield).

Synthesis of Light-Switchable Polymer (LSP)

The light-switchable hydrazone **1** (0.41 g, 1.3 mmol), NHS (0.15 g, 1.3 mmol) and EDC·HCl (0.27 g, 1.43 mmol) were dissolved in 5 mL dimethylsulfoxide (DMSO). The mixture was stirred overnight at rt under nitrogen in the dark. Then, mPEG-PELG (0.5 g, 1.3 mmol of amine) and several drops of triethylamine were added to the solution, which was then stirred for 24 h. **LSP** was obtained by dialysis (MWCO 3.5 kDa) and lyophilization (68% yield).

2.2 Nanoparticle Fabrication

The light-switchable nanoparticles (**LSNP**) were prepared using dialysis. **LSP** (5 mg) was dissolved in DMSO (1 mL), and then added dropwise into deionized water (DMSO/water = 1:10) while stirring. The nanoparticles were formed by dialyzing the solution against deionized water. The doxorubicin (DOX)-loaded **LSNP** were prepared by simultaneously dissolving **LSP** and DOX in DMSO before adding to water.

2.3 Light-Triggered Drug Release

To directly assess the light-triggered drug release, the DOX-loaded **LSNP** were placed into ultrafiltration tubes (MWCO 3 KDa) with PBS buffer and kept at 37 ℃ in an incubator with a shaking speed of 100 cycles min^{-1}. One set of tubes was irradiated at 450 nm light for specified time periods (0-30 min), the other group was kept in the dark. The fluorescence emission spectra were measured from the buffer after every irradiation using excitation wavelength of 505 nm. To quantitatively determine the amount of drug released, one tube was irradiated with 450 nm light for 5 min h^{-1} in the first 6 h, the other tube was kept in the dark. At selected time intervals, from 0.5 to 48 h, 1 mL of PBS solution in the tube was taken out and replaced with 1 mL fresh PBS. The DOX fluorescence was measured by FluoroMax-3. The cumulative amount of released DOX was calculated, and the percentages of released DOX were plotted against time.

2.4 Intracellular Photoisomerization

Confocal microscopy was used to study the intracellular photoisomerization of nanoparticles. MDA-MB-231 cells were seeded into petri dishes (35 mm × 10 mm, Corning Inc.) at a density of 10×10^4 cells/dish and allowed to grow for 24 h. Then the culture medium was replaced with a medium containing **LSNP** (12.5 μg mL^{-1}). The dish was kept under dark for 3 h, then irradiated using 450 nm light for 30 min. The images were taken at different time points under the excitation wavelength of 430 nm using a Zeiss LSM 800 confocal microscope.

2.5 Light-Triggered Cellular Uptake

Fluorescence microscopy was used to observe the light-triggered cellular uptake of DOX-loaded **LSNP**. MDA-MB-231 cells were seeded into petri dishes at a density of 10×10^4 cells/dish and allowed to grow for 24 h. Then the culture medium was replaced with the medium containing DOX-loaded **LSNP** (DOX-equivalent dose: 1 μg mL^{-1}). One dish was kept under dark for 60 min, the other dishes were irradiated with 450 nm light for 5, 10, 20 and 30 min and subsequently incubated in the dark for 55, 50, 40 and 30 min, respectively. Then the cells were washed with PBS, fixed by 2.5% paraformaldehyde, stained with 4',6-diamidino-2-phenylindole (DAPI), and imaged by fluorescence microscopy (Olympus IX73). DAPI (blue) and DOX (red) were excited at 340 nm and 485 nm, respectively.

2.6 Intracellular Drug Release

Confocal microscopy was applied to further observe the intracellular drug release of DOX-loaded **LSNP** after photoisomerization. MDA-MB-231 cells were seeded into petri dishes at a density of 10×10^4 cells/dish and allowed to grow for 24 h. Then the culture medium was replaced with the medium containing DOX-loaded **LSNP** (DOX-equivalent dose: 1 μg mL^{-1}). One dish was kept under dark for 3 h incubation, the other one was irradiated with 450 nm light for 30 min after 3 h in dark. Then the cells were washed with PBS, fixed by 2.5% paraformaldehyde, stained with DAPI, and imaged using confocal microscopy. **LSNP** (green), DOX (red) and DAPI (blue) and were excited at 430 nm, 485 nm and 340 nm, respectively.

2.7 Cytocompatibility Assay

AlamarBlue assay was used to evaluate the cytocompatibility of the nanoparticles. MDA-MB-231 human breast adenocarcinoma cells were seeded into 48-well plates at a density of 1×10^4 cells/well and allowed to grow for 24 h. Then the culture medium was replaced with the medium containing various concentrations of **LSNP** (50 μg mL^{-1} to 1000 μg mL^{-1}). One plate was irradiated with 450 nm light for 5 min/h for the first 6 h, the other plate was kept in the dark. After 48 h of co-incubation, cells were washed by PBS and treated with 300 μL of alamarBlue solution (10% alamarBlue, 80% media 199 (Gibcos), and 10% FBS, v/v) for 3 h. Then 200 μL of alamarBlue solution was transferred into a 96-well plate, which was read on a Synergy HT fluorescent plate reader (BioTek Instruments Inc., Winooski, VT, USA) at an adsorption wavelength of 570 nm. The cell viability was calculated according to the optical density (OD) value of alamarBlue at 570 nm.

2.8 Cell Cytotoxicity

AlamarBlue assay was applied to evaluate the cytotoxicity of DOX-loaded **LSNP** against MDA-MB-231 cells. MDA-MB-231 cells were seeded into 48-well plates at a density of 1×10^4 cells/well and

allowed to grow for 24 h. Then the culture medium was replaced with the medium containing various concentrations of DOX-loaded **LSNP** (DOX-equivalent dose: 0.01 μg mL^{-1} to 10 μg mL^{-1}). One plate was irradiated with 450 nm light for 5 min h^{-1} for the first 6 h, the other plate was kept in dark. 48 h later, cells were washed with PBS, incubated with 300 μL of alamarBlue solution for further 3 h, and read on a Synergy HT fluorescent plate reader to calculate the cell viability.

3 NMR Characterization

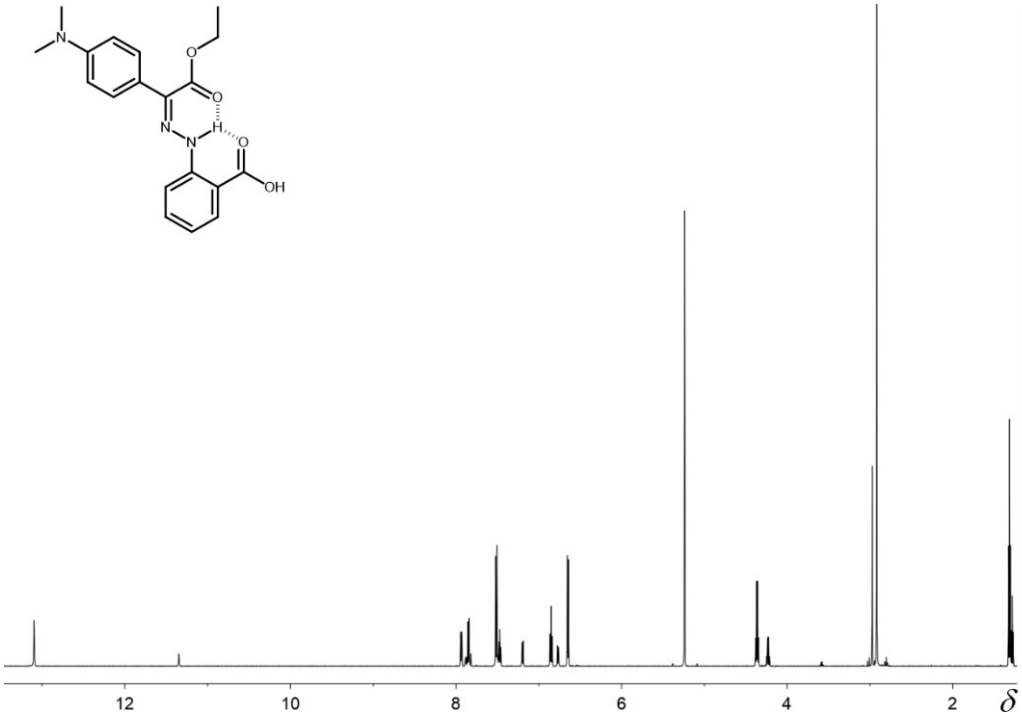

Fig. S1 ^{1}H NMR spectrum of **1** in CD_2Cl_2 (*Z*/*E*=8/2).

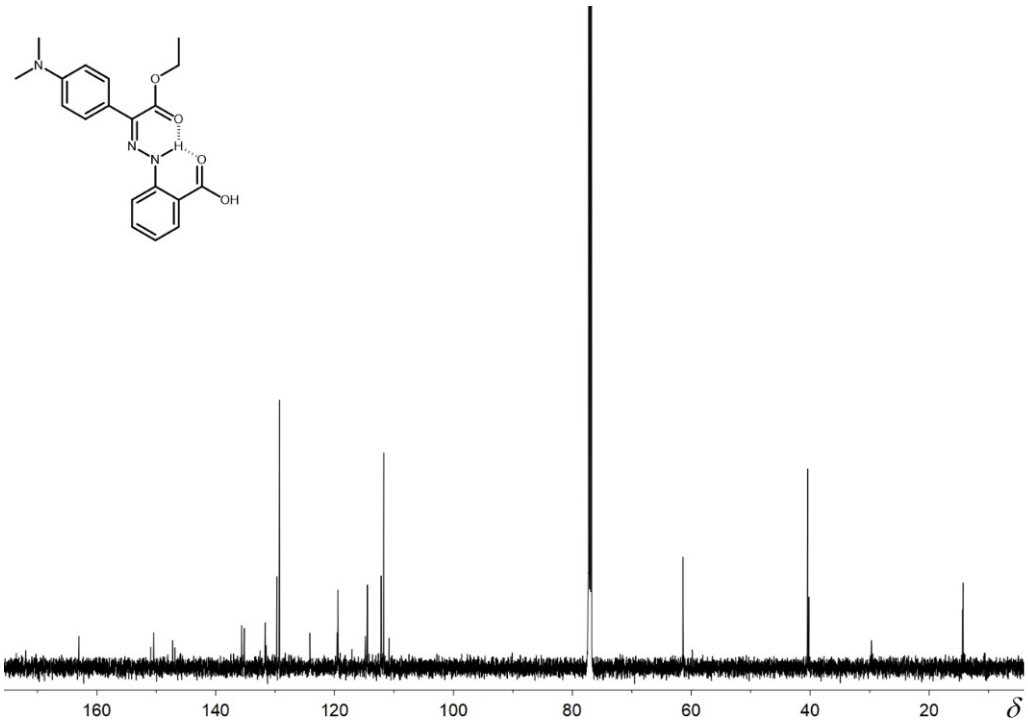

Fig. S2 ^{13}C NMR spectrum of **1** in $CDCl_3$.

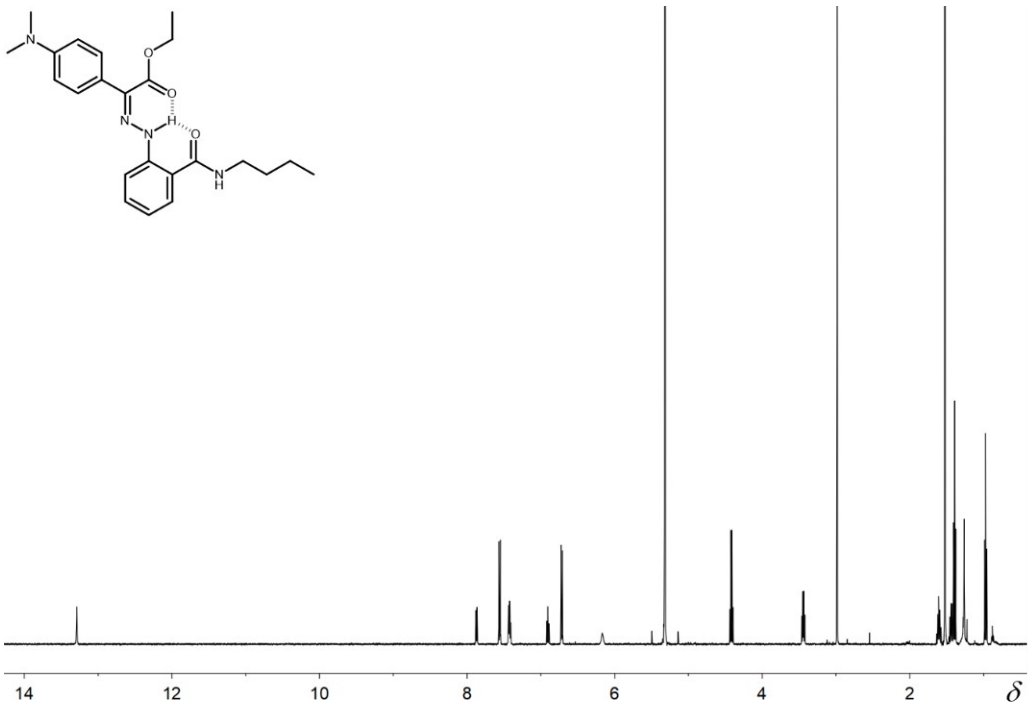

Fig. S3 ^{1}H NMR spectrum of **2** in CD_2Cl_2.

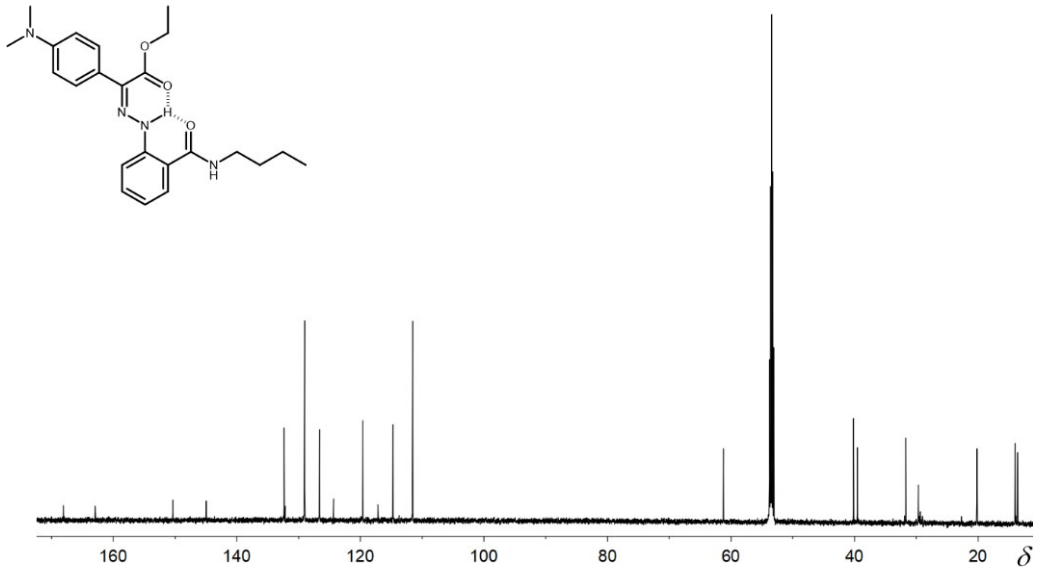

Fig. S4 ^{13}C NMR spectrum of **2** in CD_2Cl_2.

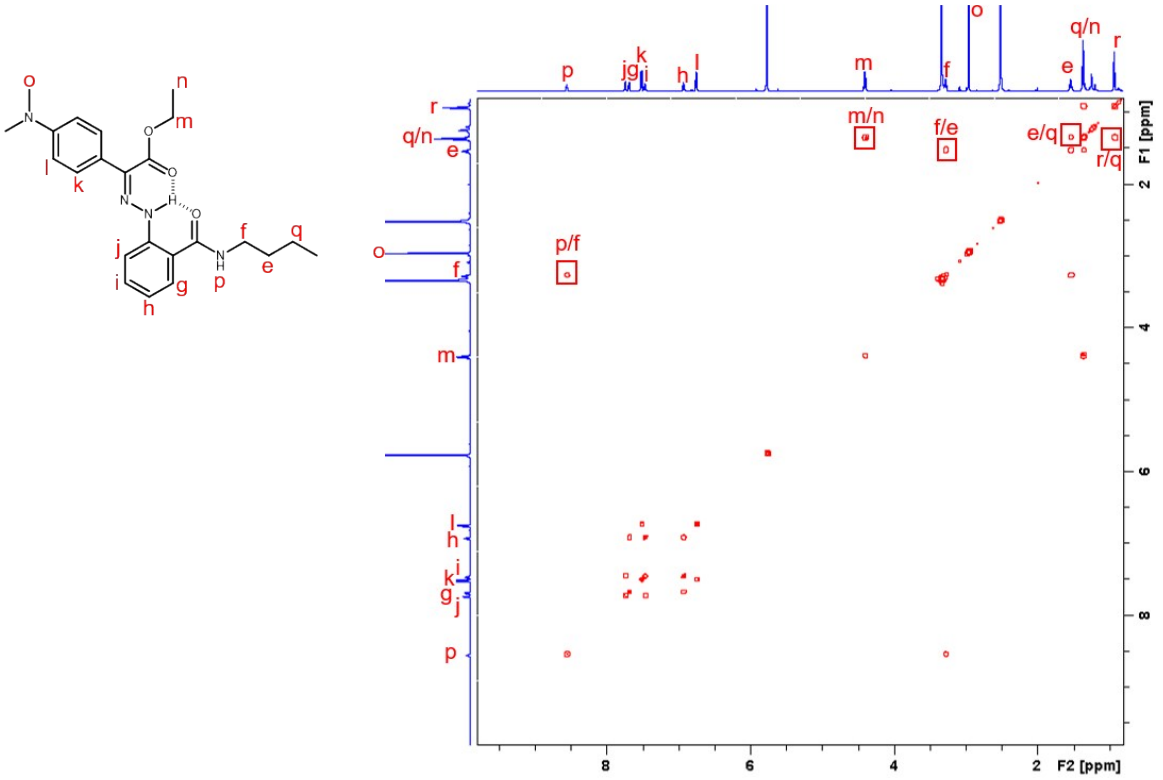

Fig. S5 2D COSY of **2** in DMSO-d_6.

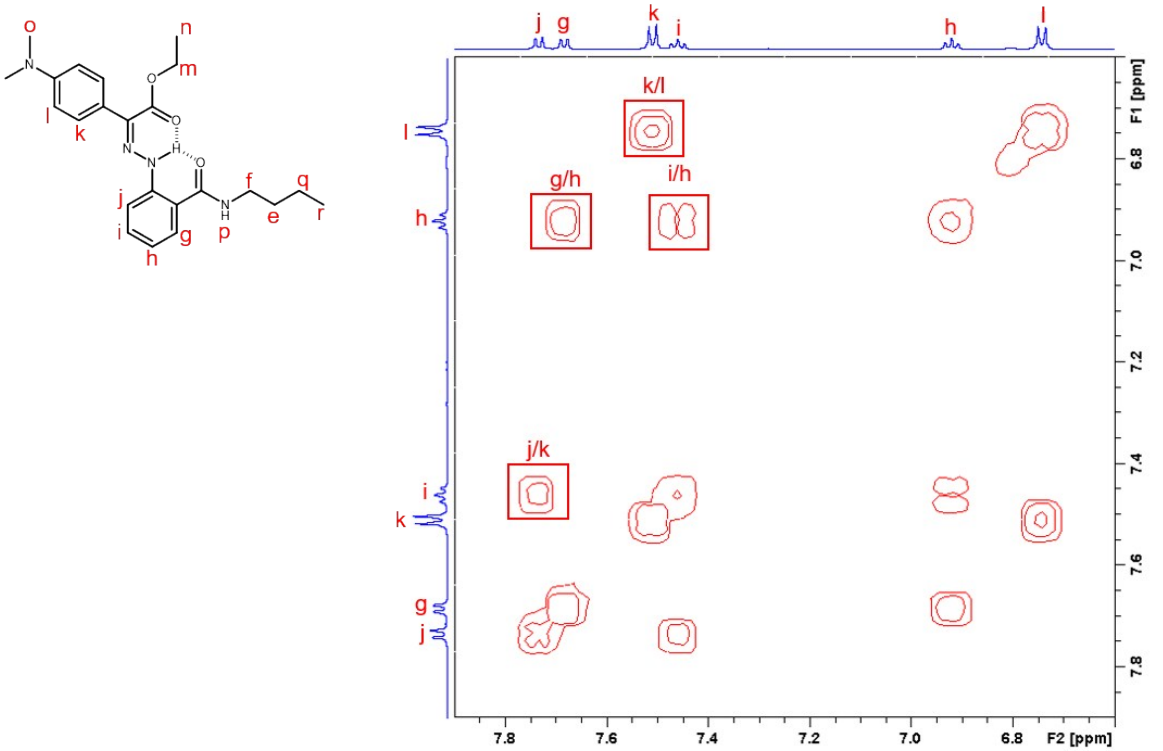

Fig. S6 Partial 2D COSY of **2** in DMSO-d_6.

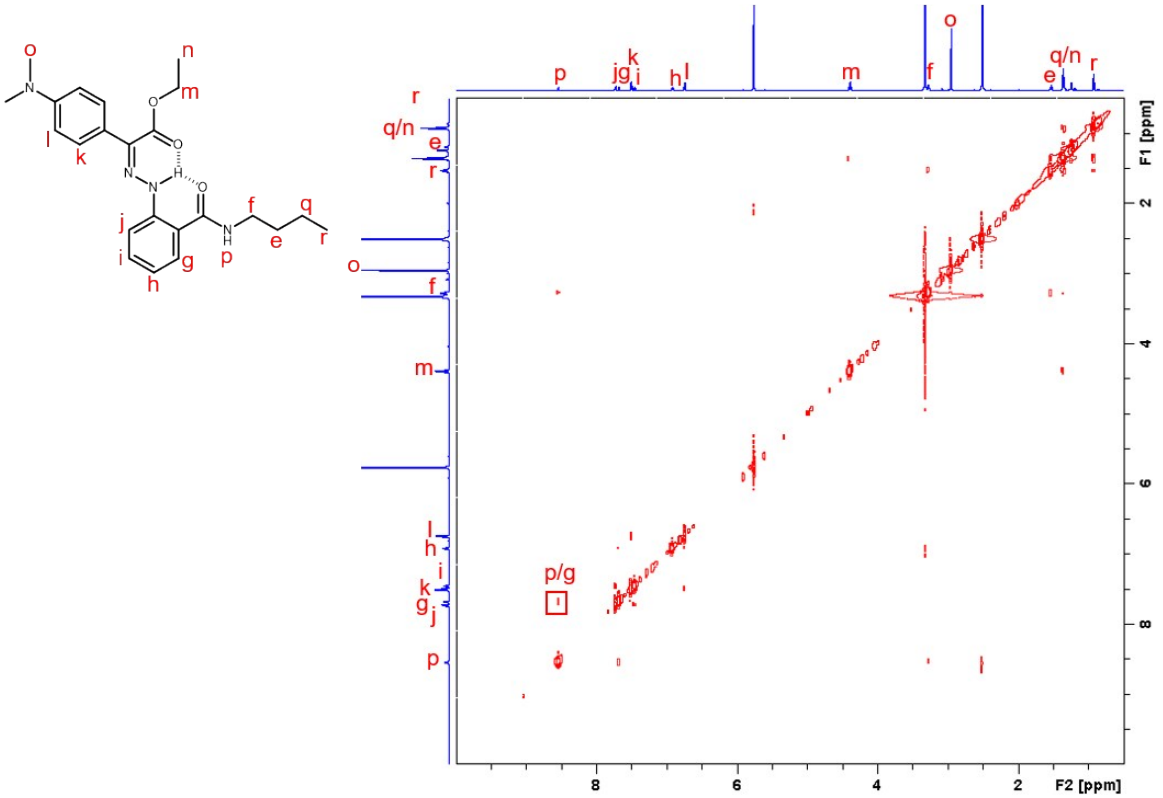

Fig. S7 2D NOESY of **2** in DMSO-d_6.

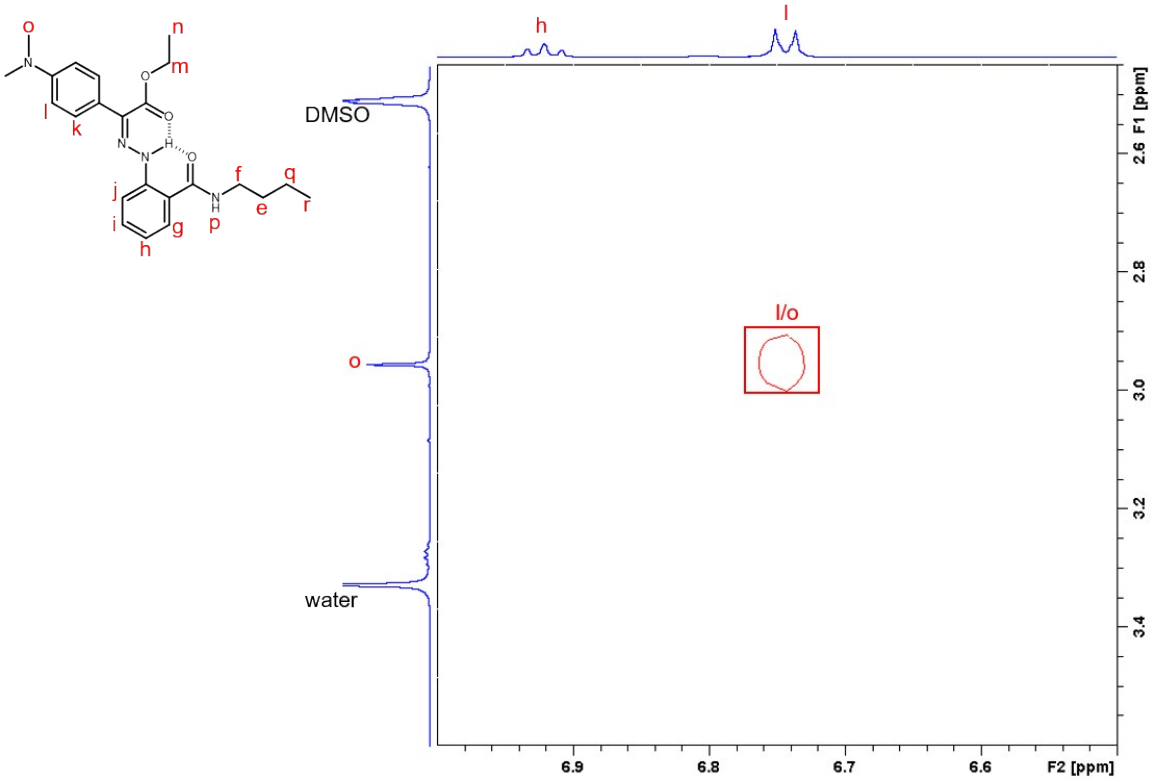

Fig. S8 Partial 2D NOESY of **2** in DMSO-d_6.

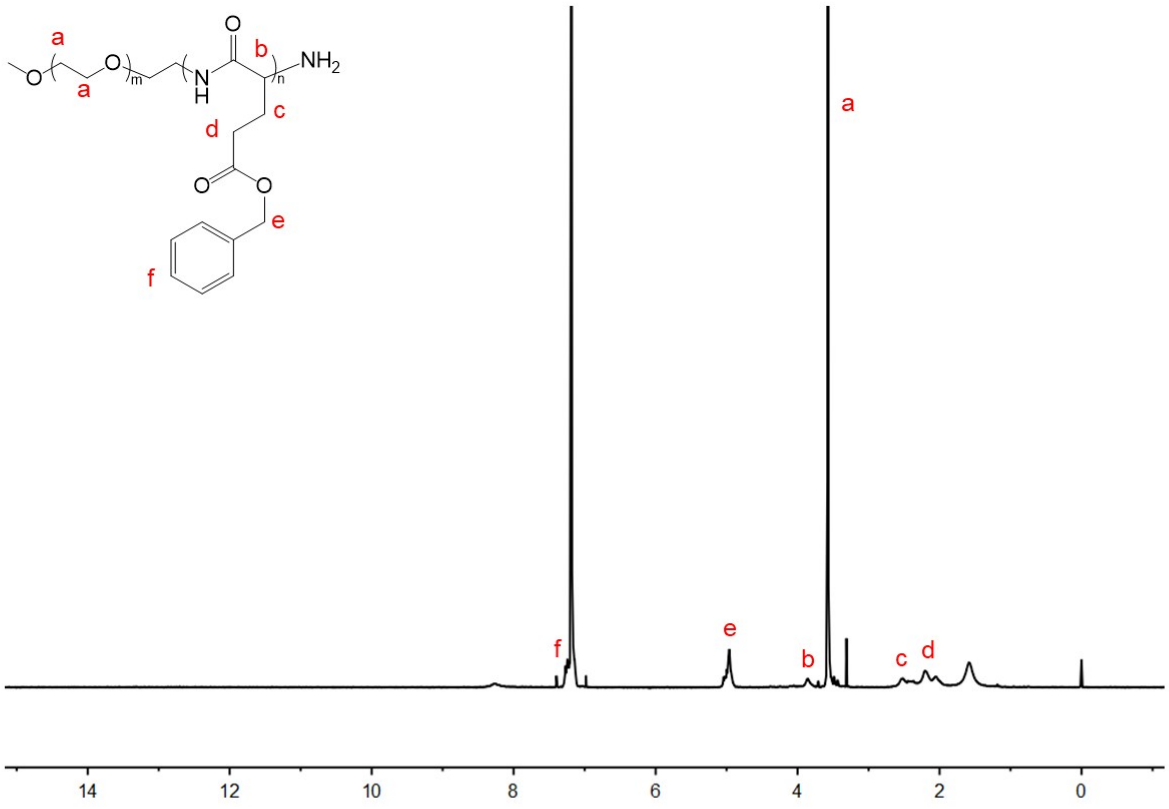

Fig. S9 ^{1}H NMR spectrum of mPEG-PBLG in $CDCl_3$.

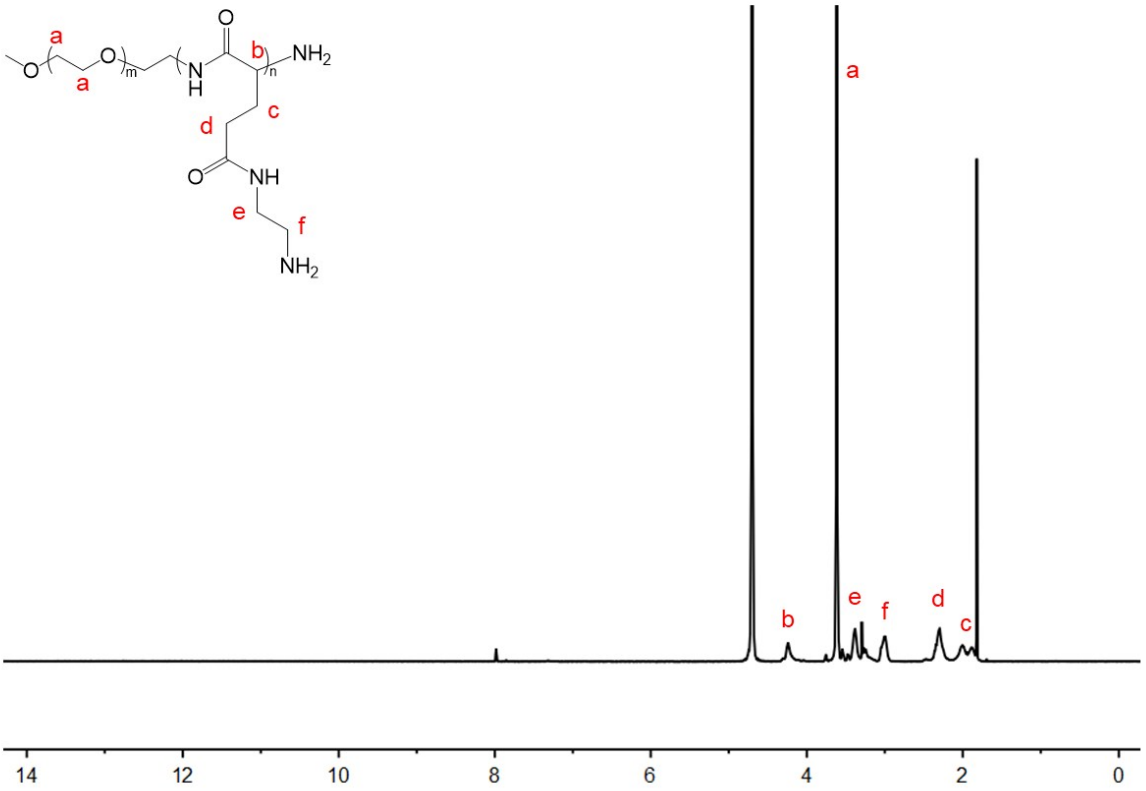

Fig. S10 ^{1}H NMR spectrum of mPEG-PELG in D_2O.

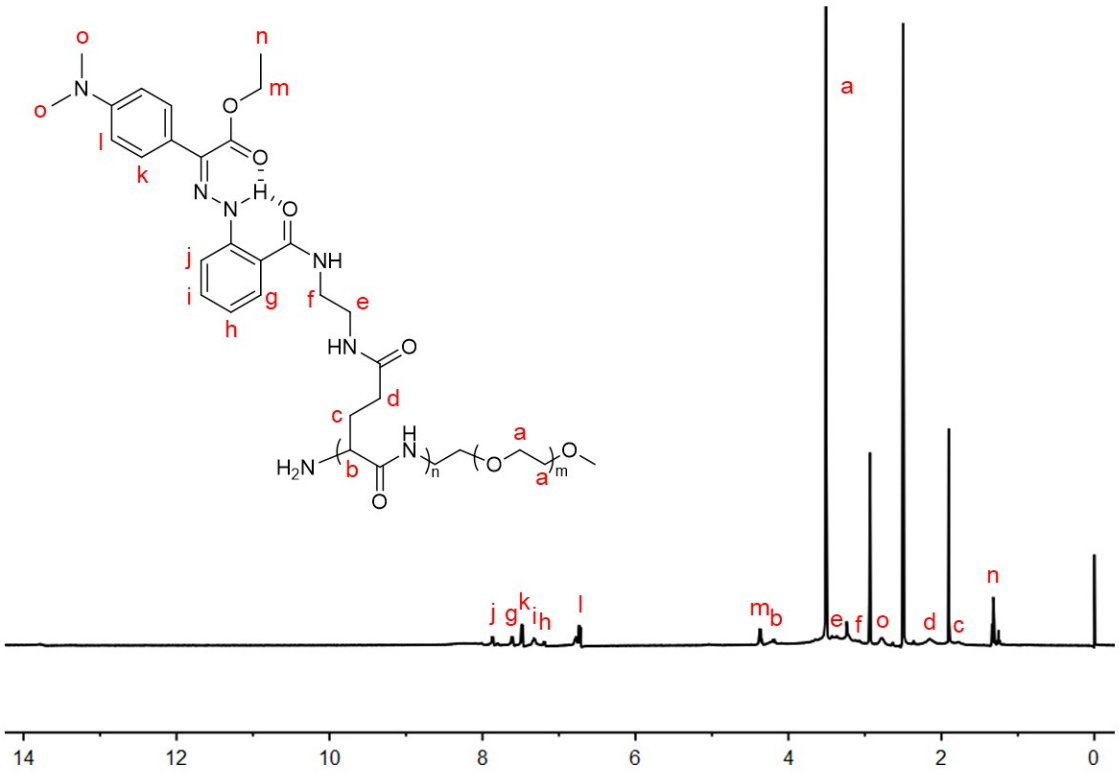

Figure S11. ^{1}H NMR spectrum of **LSP** in DMSO-d_6.

4 Photoisomerization Studies

UV-Vis spectroscopy was employed to study the photoisomerization of the hydrazone switches. Spectrophotometric grade solvents were used for the absorption studies. Hydrazone switch solutions (3.0 mL, 1.0×10^{-5} M) in DMSO were prepared and transferred into 1.0 cm quartz cuvettes for immediate UV-Vis absorption measurements. The solutions were then irradiated and corresponding UV spectra recorded. Isomerization cycles were measured by alternating the irradiation wavelength between the appropriate values and monitoring the changes in UV-Vis absorption. Photostationary states (PSS) was determined from the UV-Vis spectra collected for **2**-*Z*, and PSSs reached upon 442 and 340 nm light irradiation. [1]

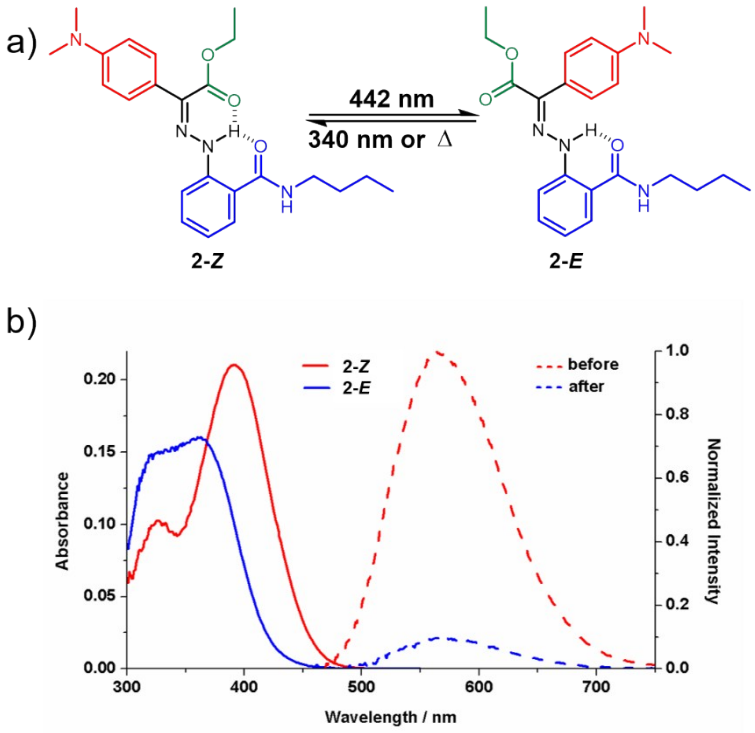

Fig. S12 (a) Light-induced *E*/*Z* photoisomerization of model compound **2**. (b) Solid lines: UV-Vis spectra (1×10^{-5} M) of **2**-*Z* and **2**-*E* in DMSO; Dashed lines: fluorescence spectra (1×10^{-5} M; λ_{ex} = 430 nm) of **2** in DMSO, before (red) and after (blue) irradiation.

We first studied the photoisomerization and emission properties of the model compound (**2**) using UV-Vis and fluorescence spectroscopies. **2**-*Z* in DMSO shows an absorption maximum (λ_{max}) at 391 nm, which shifts hypsochromically to λ_{max} = 363 nm upon 442 nm light irradiation (Fig. S12b). The reverse $E \rightarrow Z$ isomerization can be triggered using a 340 nm light source, and the process can be cycled between the two isomers by alternate irradiation of 442 and 340 nm light (Fig. S16 and S17). The $Z \rightarrow E$ photoswitching has a quantum yield ($\Phi_{Z \rightarrow E}$) of 14.0 ± 1.2 % and yields a photostationary state (PSS)

containing 91% of **2**-*E* (Fig. S13, S14 and S19). Irradiating the *E*-rich solution with 340 nm light gives rise to a PSS_{340} consisting of 77% of **2**-*Z* (Fig. S15), with a quantum yield ($\Phi_{E\rightarrow Z}$) of 8.3 ± 0.2 % (Fig. S20). The thermal $E\rightarrow Z$ relaxation half-life of **2** was determined to be 2476 ± 122 years (Fig. S21). Upon excitation (λ_{ex}) at 430 nm, the DMSO solution of **2**-*Z* exhibits an intense emission band (λ_{em}) at 564 nm, with a fluorescence quantum yield of 1.1 ± 0.1 % (Fig. S12b). Switching **2**-*Z* to **2**-*E* using 442 nm light results in emission quenching, though not complete since a certain amount of *Z* isomer (~9%) still persists at PSS (Fig. S14). The quenched emission can be restored upon irradiation with 340 nm light (Fig. S18).

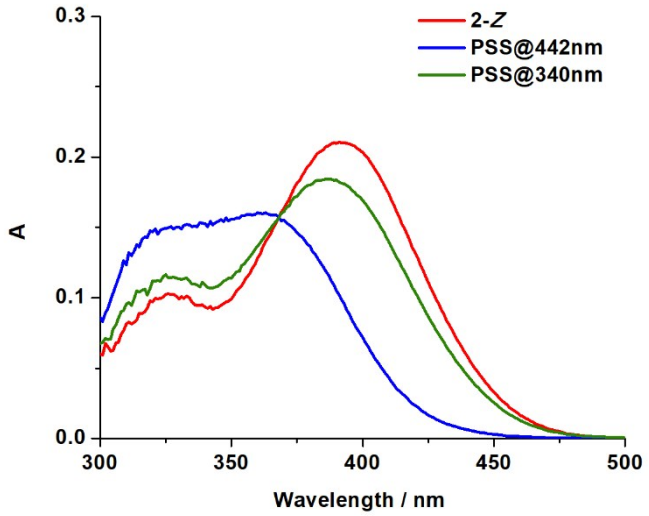

Fig. S13 UV-Vis spectra of **2**-*Z* (1.0×10^{-5} M) and PSSs (at 442 and 340 nm) in DMSO.

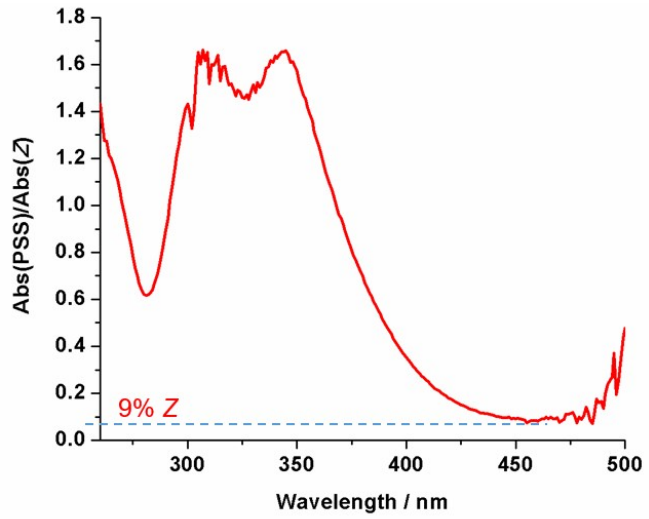

Fig. S14 The plot of Abs (PSS_{442})/Abs (*Z*) ratio *versus* wavelength from which the PSS_{442} was calculated to be 91% *E*.[1]

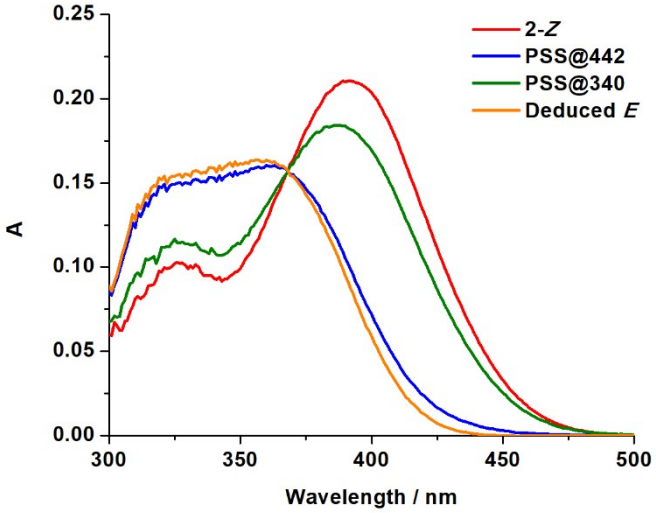

Fig. S15 The absorption spectrum of **2**-*E* (orange) was calculated using the equation: Abs (*E*) = (Abs (PSS@442 nm)-*Z*% × Abs (*Z*))/*E*%, where *Z*% and *E*% refer to the percentages of *Z* and *E* isomers at the photostationary state obtained under 442 nm light irradiation (*i.e.*, 91% of **2**-*E* and 9% of **2**-*Z*). The PSS_{340} was then calculated to be of 77% *Z* and 23% *E*. [1]

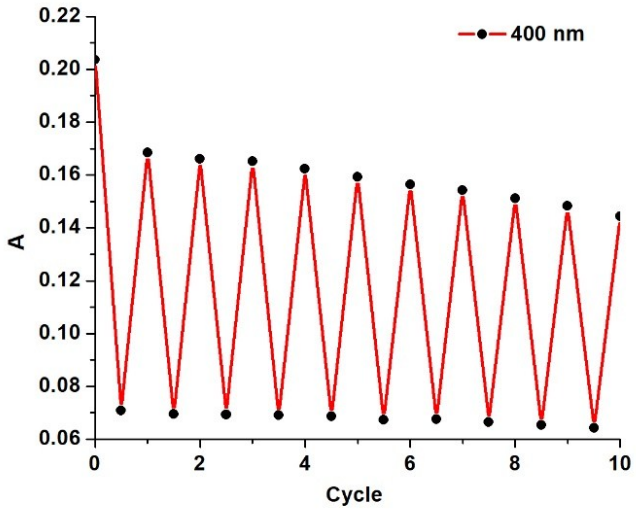

Fig. S16 Photoisomerization cycles of hydrazone switch **2** (1×10^{-5} M) in DMSO at 294 K. The absorbance change at 400 nm was monitored while alternating the irradiation wavelength between 442 and 340 nm.

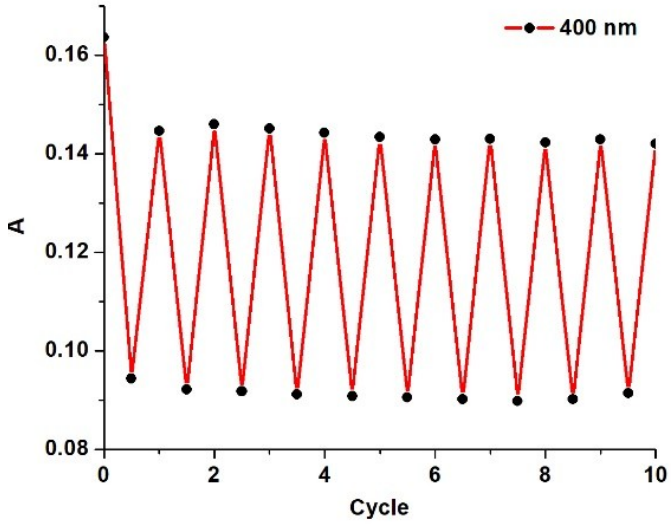

Fig. S17 Photoisomerization cycles of hydrazone switch **2** (1×10^{-5} M) in DMSO/water (1:1) at 294 K. The absorbance change at 400 nm was monitored while alternating the irradiation wavelength between 442 and 340 nm.

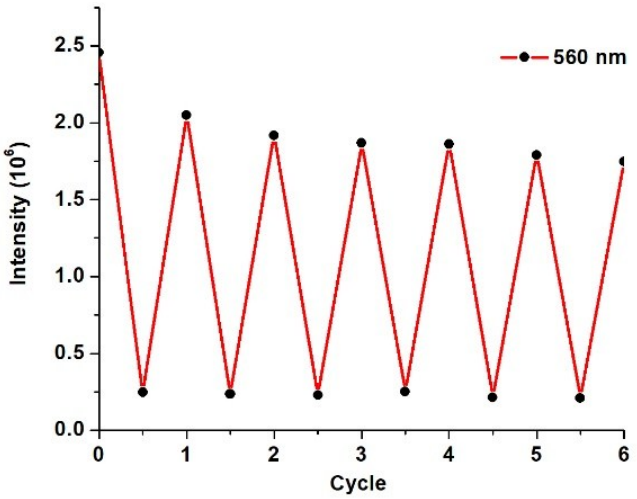

Fig. S18 Fluorescence switching cycles of hydrazone switch **2** (5×10^{-6} M) in DMSO at 294 K. The emission change at 560 nm was monitored while alternating the irradiation wavelength between 442 and 340 nm (λ_{ex} = 430 nm).

5 Photoisomerization Quantum Yield

The molar photon flux I_0 at 340 and 442nm were determined using chemical actinometry.[2] A 0.002 L (= V_0) solution of potassium ferrioxalate in 0.05 M H_2SO_4 was placed in an 1.0 cm cuvette and irradiated for 30 s (= t_0). The irradiated solution was combined with 3.5 equiv. of ferrozine, and stirred under dark for an hour. The resulting solution, containing reddish-purple $[Fe(ferrozine)_3]^{2+}$ complex was diluted by a factor of 30 (= n), and its absorbance was measured at 563 nm (A_{563}), where its molar absorption coefficient (ε_{563}) is 27,900 cm^{-1} M^{-1}. The molar photon flux I_0 of the light source at different wavelength was determined using Equation 1.

$$I_0\left(quanta \cdot s^{-1}\right) = \frac{A_{563} \cdot n \cdot N_A \cdot V_0}{\varepsilon_{563} \cdot l \cdot t_0 \cdot \phi_\lambda} \qquad \text{Equation 1}$$

where l indicates the length of the cuvette, and ϕ_λ stands for the quantum yield of the photo-reduction of Fe(III) oxalate induced by the light source (ϕ_{340} = 1.25 and ϕ_{442} = 1.11).

The photoisomerization quantum yield of hydrazone **2** was measured according to a previously reported methods.[3]

$$A \underset{k_r}{\overset{k_f}{\rightleftharpoons}} B$$

In a photochemical reaction, species A absorbs light to generate the product B.
The rate law for the formation of species ***A*** is as follow:

$$C_A = \frac{C_{total} \cdot k_r}{k_f + k_r} + \frac{C_{total} \cdot k_f}{k_f + k_r} e^{-(k_f + k_r)t} \qquad \text{Equation 2}$$

C_A is proportional to the absorbance of species ***A***. An exponential fit of absorbance as a function of time gives the observed rate constant $k_{obs} = k_f + k_r$. For hydrazone switch **2**, the thermal relaxation is extremely slow at room temperature (Fig. S21) and so $k_{A \to B} \approx k_{obs.}$

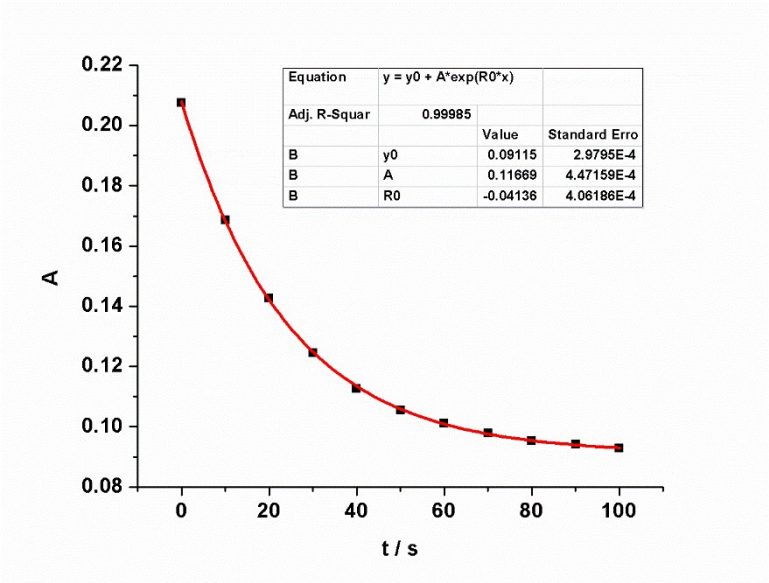

Fig. S19 Kinetics for the photoisomerization (irradiation at 442 nm) of **2**-*Z* to **2**-*E* in DMSO (1×10^{-5} M) at 298 K; the plot is of the absorption (λ_{max} = 391 nm) of **2**-*Z* at a function of time. $\varepsilon_{\mathbf{2}\text{-}Z@442nm}$ = 5200 $M^{-1}\cdot cm^{-1}$ was used for quantum yield calculations. The photoisomerization quantum yield was calculated to be 14.0 ± 1.2% based on three consecutive measurements.

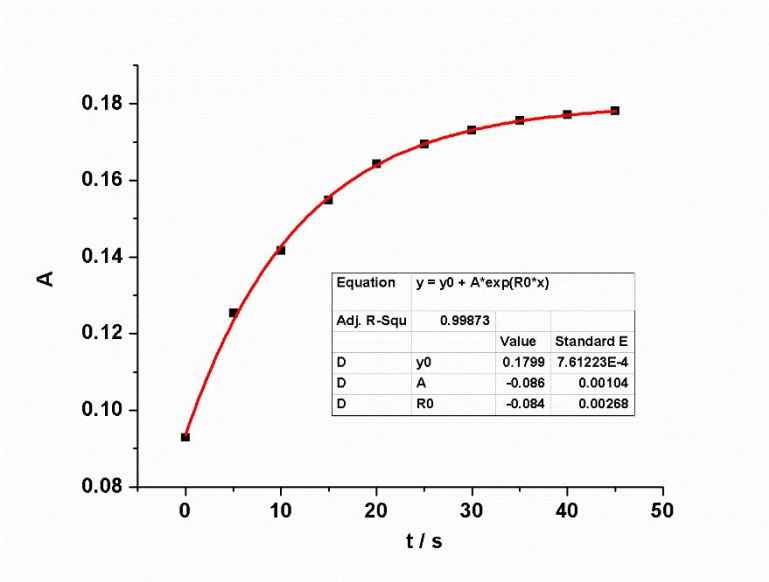

Fig. S20 Kinetics for the photoisomerization (irradiation at 340 nm) of **2**-*E* to **2**-*Z* in DMSO (1×10^{-5} M) at 298 K; the plot is of the absorption (λ_{max} = 391 nm) of **2**-*Z* at a function of time. $\varepsilon_{\mathbf{2}\text{-}E@nm}$ = 15800 $M^{-1}\cdot cm^{-1}$ was used for quantum yield calculations. The photoisomerization quantum yield was calculated to be 8.3 ± 0.2% based on three consecutive measurements.

6 Kinetic Studies

The thermal isomerization kinetics of hydrazone switch **2**-*Z* at 408 K was studied using ^{1}H NMR spectroscopy. Solutions of **2**-*Z* (~10^{-3} M) in DMSO-d_6 were irradiated at 442nm wavelength and then left in a Haake F3 circulating oil bath at a preset temperature. ^{1}H NMR spectra were acquired at different intervals at room temperature to monitor the change in the ester CH_2 proton signal intensity as a function of time. The change in intensity of the ester CH_2 protons were used to calculate the ratio of the *Z* and *E* isomers. The thermal isomerization rates (k_1) were determined by least-square curve fittings using an integrated and combined rate equation (Equation 5) of a single-species reversible reaction: [4]

$$\mathbf{A} \underset{k_{-1}}{\overset{k_1}{\rightleftharpoons}} \mathbf{Z}$$

$$K_{eq} = \frac{k_1}{k_{-1}} = \frac{C_{\mathrm{A}}^0 - C_{\mathrm{A}}^{eq}}{C_{\mathrm{A}}^{eq}} \qquad \text{Equation 3}$$

$$\ln\left(\frac{C_{\mathrm{A}} - C_{\mathrm{A}}^{eq}}{C_{\mathrm{A}}^0 - C_{\mathrm{A}}^{eq}}\right) = -\left(k_1 + k_{-1}\right)t \qquad \text{Equation 4}$$

Combining Equation 3 and 4 will give Equation 5 as follow,

$$C_{\mathrm{A}} = \left(C_{\mathrm{A}}^0 - C_{\mathrm{A}}^{eq}\right) \times e^{\left(\frac{-k_1 \cdot C_{\mathrm{A}}^0 \cdot t}{C_{\mathrm{A}}^0 - C_{\mathrm{A}}^{eq}}\right)} + C_{\mathrm{A}}^{eq} \qquad \text{Equation 5}$$

where C_{A}, C_{A}^0, and $C_{\mathrm{A}}^{\mathrm{eq}}$ stand for experimental, initial, and equilibrium concentrations of the metastable configuration of the hydrazone switch, respectively; *t* stands for the thermal relaxation time.

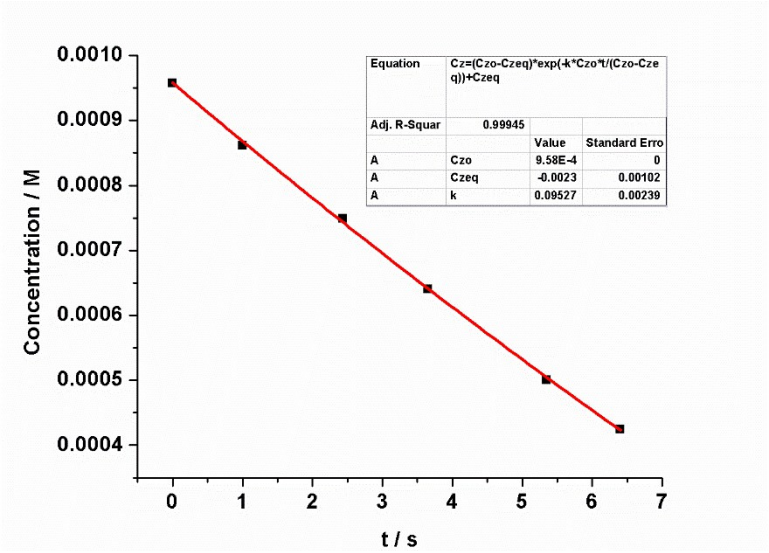

Fig. S21 Thermal isomerization of **2**-*E* → **2**-*Z* in DMSO-d_6 at 408 K. The plot is of the concentration of **2**-*E* as a function of time. The resulting k_1 value was calculated to be $(2.7 \pm 0.2) \times 10^{-5}$ s^{-1} based on three consecutive measurements at this temperature. And the thermal relaxation half-life at 298 K was extrapolated to be 2476 ± 122 years following the reported method.[5]

7 Light-Triggered Size Expansion of DOX-Loaded LSNPs

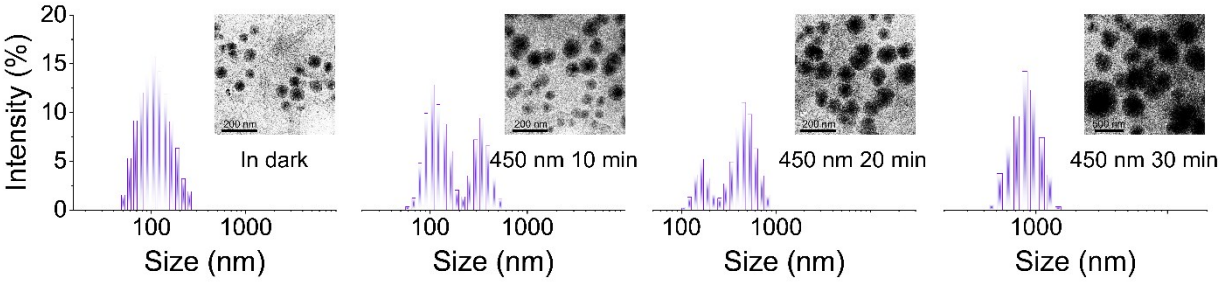

Fig. S22 DLS and TEM (inset) analyses of dox-loaded LSNPs in the dark and after applying 450 nm irradiation for the different time intervals.

8 Correlation Degree of Emission Quenching with Amount of Drug Release

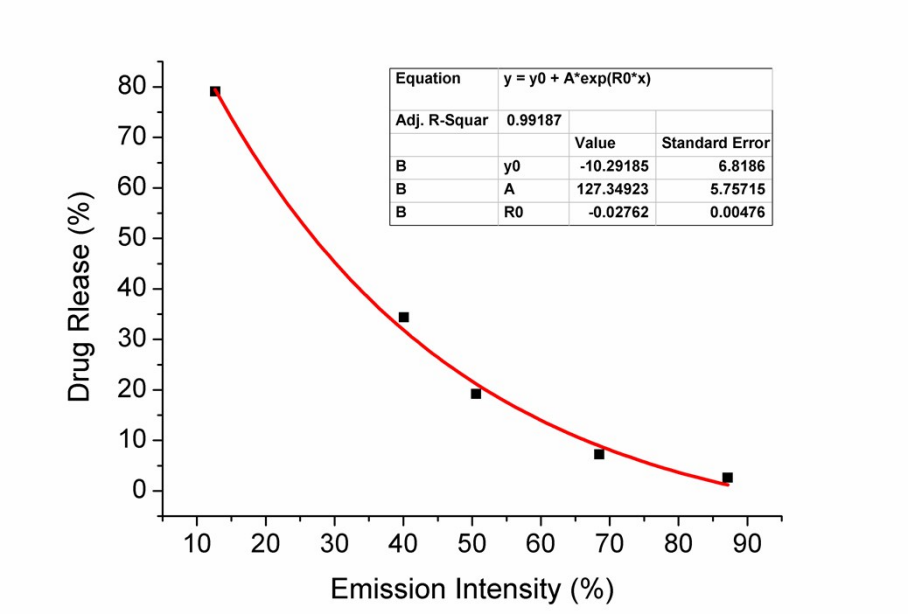

Fig. S23 The plot obtained using the data in Fig. 1b and Fig. 2a in the manuscript. The percentage of drug release after 450 nm irradiation is correlated with the degree of polymer emission quenching. The drug release amount can be calculated using Equation 6.

$$y = 127.35*\exp(-0.028*x)-10.29 \qquad \text{Equation 6}$$

9 Light-Triggered Cellular Uptake

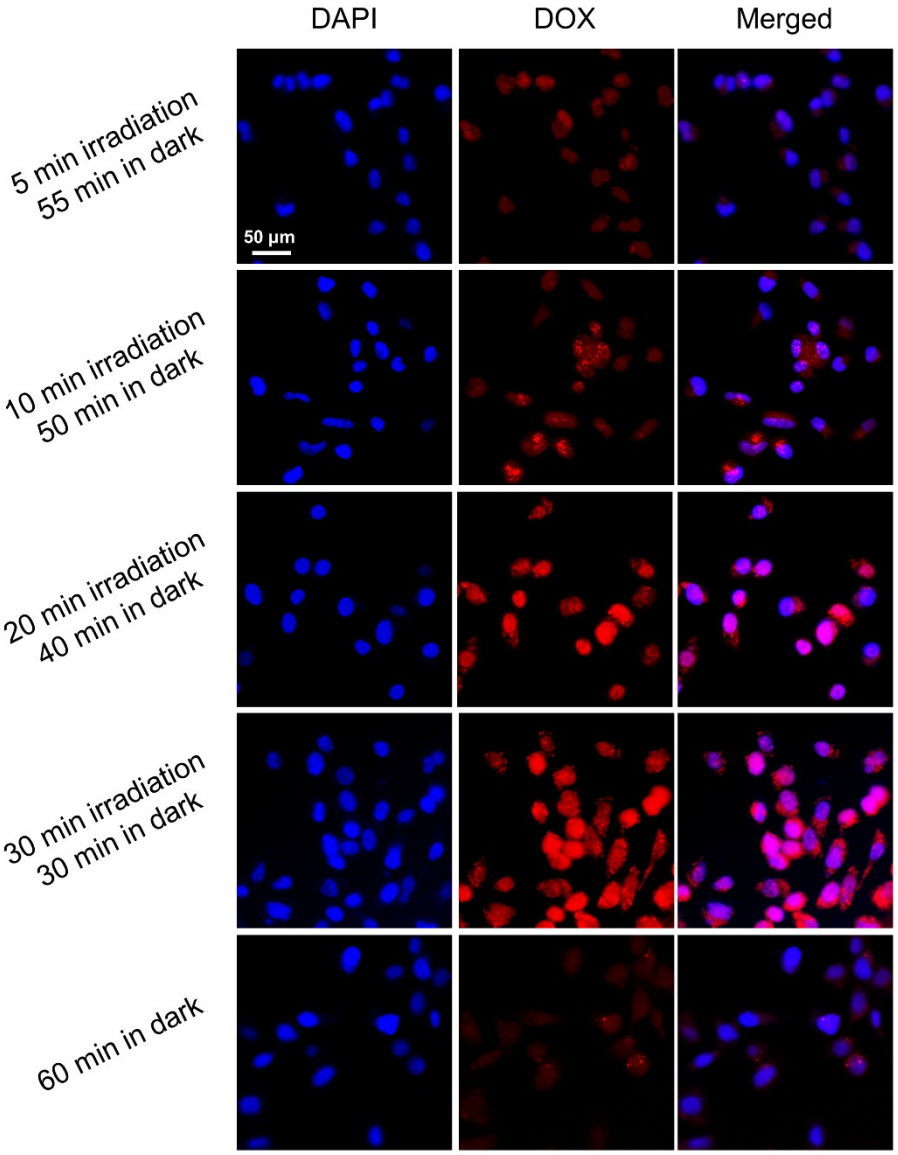

Fig. S24 Fluorescence images in MDA-MB-231 cells showing the light-triggered cellular uptake. Cells were treated with DOX-loaded **LSNP** for 450 nm irradiation and/or kept in dark as illustrated (DOX-equivalent dose: 1 μg mL^{-1}).

10 Semi-Quantatative Analysis of Intracellular Drug Release

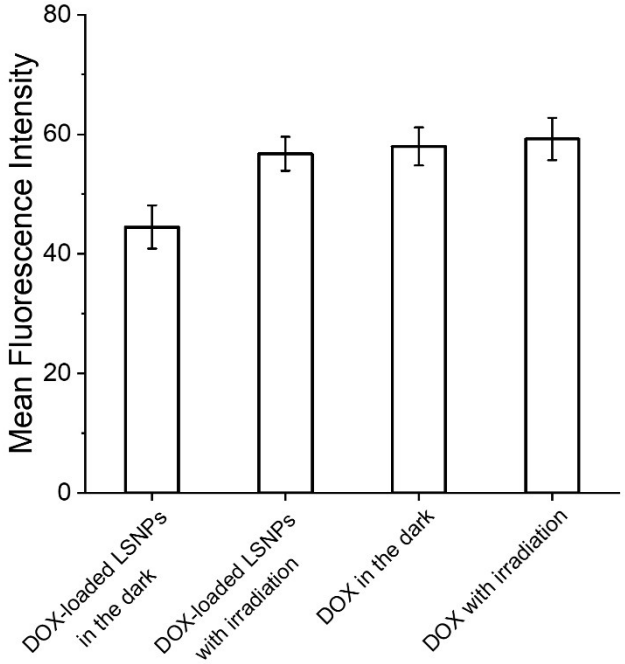

Fig. S25 Mean fluorescence intensity of DOX-loaded LSNPs and DOX incubated with MDA-MB-231 cells in the dark for 3 h or irradiating with 450 nm light for 30 min after 3 h of dark incubation. The data were measured by ImageJ 8.0.

11 Cell Cytotoxicity

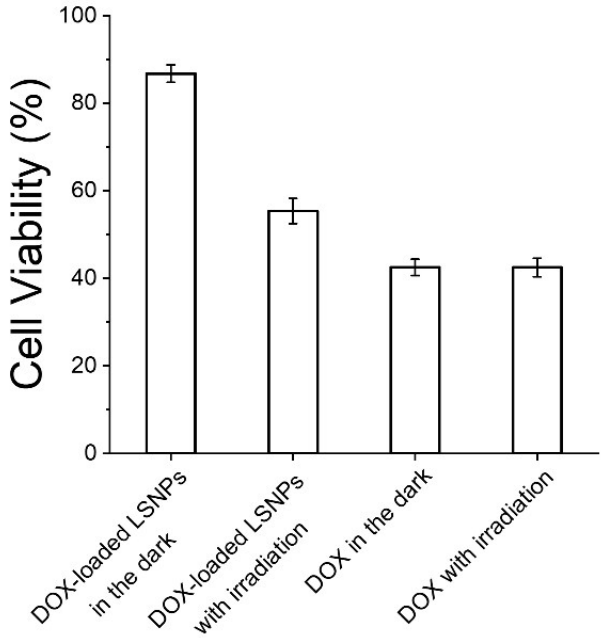

Fig. S26 Viability of MDA-MB-231 cells after treating with free DOX or DOX-loaded LSNPs in the dark or irradiation with 450 nm light (irradiation for 5 min per hour for the first 6 h) at 1 μg mL^{-1} (n = 5).

References

1. B. Shao, M. Baroncini, H. Qian, L. Bussotti, M. Di Donato, A. Credi and I. Aprahamian, *J. Am. Chem. Soc.,* 2018, **140**, 12323.
2. a) H. J. Kuhn, S. E. Braslavsky and R. Schmidt, *Pure Appl. Chem.,* 2004, **76**, 2105; b) H. M. D. Bandara, T. R. Friss, M. M. Enriquez, W. Isley, C. Incarvito, H. A. Frank, J. Gascon and S. C. Burdette, *J. Org. Chem.,* 2010, **75**, 4817.
3. H. Qian, S. Pramanik and I. Aprahamian, *J. Am. Chem. Soc.,* 2017, **139**, 9140.
4. K. A. Connors, *Chemical kinetics: the study of reaction rates in solution*; VCH: New York, 1990, pp. 60.
5. M. J. Moran, M. Magrini, D. M. Walba and I. Aprahamian, I. *J. Am. Chem. Soc.,* 2018, **140**, 13623.